20th Australasian Fluid Mechanics Conference
Perth, Australia
5-8 December 2016

Nonlinear Exact Coherent Structures in pipe flow and their instabilities

O. Ozcakir[1]

[1]School of Mathematical Sciences, Monash University, Clayton, VIC 3800, Australia

Abstract

In this paper we present results from stability calculation of travelling waves of different kinds. All, but one, of these states appear through saddle-node bifurcations. All these solutions are linearly unstable and have a low-dimensional unstable manifold. We also present numerical evidence that suggests solutions first identified by [21] exhibit Vortex-Wave Interaction discovered by [8] for large R.

Introduction

Research on flows in pipes, channels and boundary-layer flows have attracted many researchers. There has been particular interest in travelling wave (TW) states at large Reynolds number R in channel ([11], [18], [19], [20], [6], [1]) and pipe geometries ([5], [9], [21], [10], [12], [16]) with different degrees of symmetry. These states do not arise from finite R bifurcation of plane Couette or Hagen-Poiseuille flow in a pipe, though they come increasingly close as $R \to \infty$. They generally appear through saddle-node bifurcations with 'upper' and 'lower' branches. The branch with high wall shear stress (and therefore have higher energy) is called 'upper' branch, while the branch with low wall shear stress that corresponds to lower energy dissipation is called the 'lower' branch.

In pipe flow, if we use cylindrical coordinates (r,θ,z) with cylinder axis aligned along z, and nondimensionalization with domain corresponding to $r < 1$, the nonlinear states are three dimensional traveling wave solutions to Navier-Stokes equations that are of the form

$$\mathbf{u} = \mathbf{v}_P(r) + \mathbf{U}(r,\theta) + \mathbf{v}_w(r,\theta,z-ct) \qquad (1)$$

where $\mathbf{v}_P(r) = (1-r^2)\hat{\mathbf{z}}$ is Hagen-Poiseuille flow, $\mathbf{U}(r,\theta)$ is streamwise independent part of the flow and $\mathbf{v}_w = (u,v,w)$ is 2π periodic in both θ and in $\tilde{z} := \alpha(z-ct)$, with zero axial average over a period, denoted by $\langle \mathbf{v}_w \rangle = 0$. If we write $\mathbf{U}(r,\theta) = (U(r,\theta),V(r,\theta),0) + (0,0,W(r,\theta))$, the first term contains radial and azimuthal components of streamwise independent velocity $\mathbf{U}(r,\theta)$ which represents streamwise vortices and is referred to as the *roll* part of the flow; the latter is termed the *streak* and represents streamwise-independent axial velocity. The last term in (1) represents three dimensional wave part of the flow.

The amplitudes of the rolls, streaks and waves have to be just of the right size to sustain this three way interaction between rolls, streaks and waves. This three way interaction has been described completely for channel flows asymptotically by [7] through numerical solutions of the rescaled parameter free equations, and in agreement found with direct numerical calculations ([20], [1]) even at moderate R. We refer to these states as VWI (Vortex-Wave Interaction) states as it is descriptive of the physical mechanism that sustains such flows, as discovered originally by [8]. As described by large R asymptotics by [7], VWI states are characterized by small amplitude linear waves driving the rolls through Reynolds stress. Another possibility for travelling waves is the occurrence of a fully nonlinear viscous core (NVC) similar to the one observed earlier in boundary layer flows by [2]. While NVC states are also characterized by a three-way interaction mentioned before, there is no meaningful separation in scales between rolls, streaks and waves in this case, and the interaction between different axial wave number components is fully nonlinear as $R \to \infty$, unlike the VWI states.

In Ozcakir *et al.*[14], previous numerically calculated states in pipe geometry were roughly identified as finite R realizations of a VWI state with an asymptotic structure similar to the ones in channel flows studied earlier by Hall & Sherwin [7]. There is also some evidence to suggest that VWI states are edge states ([15]) for large Reynolds number in the sense that they separate the initial conditions in phase space between those that return to laminar flow from those that don't. Furthermore, when the unstable manifold of these states are low-dimensional, as suggested by earlier numerical calculations ([17]), of one of these states in pipe geometry, they correspond to exact coherent structures that are experimentally observable ([9]) in intermediate R turbulence with the flow moving slowly from one TW state to another. In the same work, a new class of TW solutions, identified as NVC states, were found similar to the one observed earlier in boundary-layer flows by Deguchi & Hall [2]. The existence and stability of such travelling wave states, and their connection in phase space play important roles in understanding both transition and large R behavior of pipe flows. These nonlinear TW states are also of potential technological importance if suitable controls can be inserted to stabilize a coherent state with a significantly smaller drag than an uncontrolled turbulent flow.

The aim of this short paper is to briefly describe already found ([14]) three different class of travelling wave solutions and present stability properties of them.

Computational Method

The TW solutions we are looking for satisfy the Navier-Stokes

$$\mathbf{u}_t + \mathbf{u}\cdot\nabla\mathbf{u} = -\nabla p + \frac{1}{R}\Delta\mathbf{u} \quad , \ \nabla\cdot\mathbf{u} = 0 \qquad (2)$$

in the form (1).

Our computational method is based on Galerkin truncation in Fourier-modes in θ and $z-ct$ and a Chebyshev representation in r similar to [21] which automatically accounts for the boundary condition. Details of numerical methods used in our calculations can be found in [14].

A similar representation is used for linear stability of equilibrium $\mathbf{u}(r,\theta,z-ct)$ states. We consider perturbations of the form $e^{\lambda t}\tilde{u}(r,\theta,z-ct)$ with growth rate λ moving at a rate c,equilibrium wavespeed. Stability analysis is performed by solving linearized Navier-Stokes equation (2) for infinitesimal small perturbation $\varepsilon e^{\lambda t}\tilde{u}(r,\theta,z-ct)$ added to the equilibrium solution. The number of unstable modes a TW has depends on the space in which the stability analysis was performed. In theory, one should allow all axial, azimuthal modes on an infinitely long pipe; however this is not possible numerically. We restrict our computations into the space in which solutions reside; i.e. $\tilde{u}(r,\theta,z-ct)$ possesses same symmetries as equilibrium solution unless we analyze stability around a bifurcation point where two equilibrium solutions meet. As in full nonlinear Navier-Stokes problem, we use Galerkin truncation in Fourier-modes in θ and $z-ct$ and a Chebyshev representation in r. Linear stability computations are done using direct or newton solver. Also, higher resolution calculations are performed by solving linear eigenvalue problem using Newton method with initial guess chosen from coarser resolution computations.

Numerical Results

Calculations described here are limited to $k_0 = 2$; i.e. two-fold azimuthally symmetric TW states. We assume TWs have S-symmetry (shift-and-reflect). In addition, a class of NVC states, identified as $C2$ possesses Ω_2-symmetry (shift-and-rotate) as defined in [13]. For $k_0 = 2$, this results in rolls and streaks having four-fold azimuthal symmetry.

The first solution we found is called WK state. Note that, in the previous paper ([14]) we were unable to get numerical convergence for WK solutions for values of R larger than about 11,000 and so agreement with asymptotic scaling results for VWI-states was only qualitative. Other solutions, $C1$ and $C2$, collapse towards the center of the pipe as $R \to \infty$. These were identified as NVC states. Despite localization of rolls and waves over a shrinking core at the center of the pipe, the streaks do not decay and remain the same size outside as inside the core, until wall effects become important.

Figure 1 shows the phase speed c as a function of R for WK, $C1$ and $C2$ solutions at axial-wave speed $\alpha = 1.55$. In [14], WK solutions were shown upto $R = 11,000$ and $C1$, $C2$ solutions were only displayed for the lower-branch since lower branch asymptotics were investigated. Here, we extend our computations to WK solutions for larger R and the upper-branch $C1$-$C2$ solutions.

In figures 2, 3 and 4 we display roll, streak and wave components of these TW states in a plane perpendicular to the pipe axis at $R = 50000$ when $\alpha = 1.55$. In each plot the rolls $(U,V,0)$, radial and azimuthal waves $(u,v,0)$ are depicted using arrows whilst the axial velocity intensity of streaks W and axial waves w are represented in colors where the lighter color corresponds to positive values of W and w, while darker colors correspond to negative such values. Axial wave velocity $w(r,\theta,z_0)$ is shown at a fixed $z_0 = 2\pi/\alpha$. It is clear from figure 2b that, most action of waves are occurring around a small region which is consistent with VWI theory. On the other hand, roll, wave actions of $C1$ and $C2$ solutions are concentrated at the core while streaks are roughly the same size outside the core.

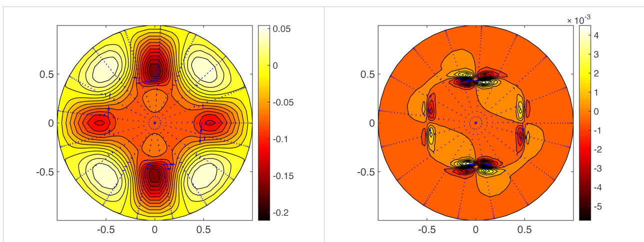

(a) $\mathbf{U}(r,\theta)$ (b) $\mathbf{v}_w(r,\theta,z_0)$

Figure 2: (a)Roll $(U,V,0)$, streak $(0,0,W)$ and (b) (u,v,w) wave profiles at $R = 50000$ for WK at $\alpha = 1.55$. 15 equispaced contour levels are plotted between minimum and maximum (a) $W(r,\theta)$and (b) $w(r,\theta,z_0)$ where min/max taken over (r,θ).

In figure 5 some results on Reynolds stresses S_1 and S_2 as defined in [14] are shown. The contours of $\frac{S_2}{S_{2,m}}$ in figure 5a appear accumulated around the critical curve (where $1-c-r^2+W(r,\theta)=0$) shown in black as expected from VWI states. Figure 5b shows $S_{j,m} := \max_{(r,\theta)} S_j(r,\theta)$ at $j = 1,2$ against R for $\alpha = 1.55$ for WK solutions. Linear fittings(dotted-line) involved the range $1.2\times10^4 < R < 5\times10^4$. $S_{1,m}$, $S_{2,m}$ scale as $R^{-1.58}$, not very close to asymptotic scaling $R^{-5/3}$ of VWI states. However, it is clear that, as R increases both $S_{2,m}$ and $S_{1,m}$ curves (solid lines) become steeper suggesting that R is still not large enough to reach the asymptotic scaling regime.

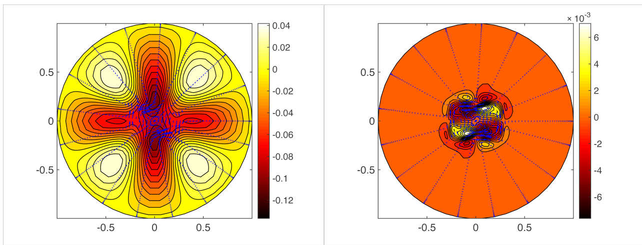

(a) $\mathbf{U}(r,\theta)$ (b) $\mathbf{v}_w(r,\theta,z_0)$

Figure 3: (a)Roll $(U,V,0)$, streak $(0,0,W)$ and (b) (u,v,w) wave profiles at $R = 50000$ for $C1$ at $\alpha = 1.55$. 15 equispaced contour levels are plotted between minimum and maximum (a) $W(r,\theta)$and (b) $w(r,\theta,z_0)$ where min/max taken over (r,θ).

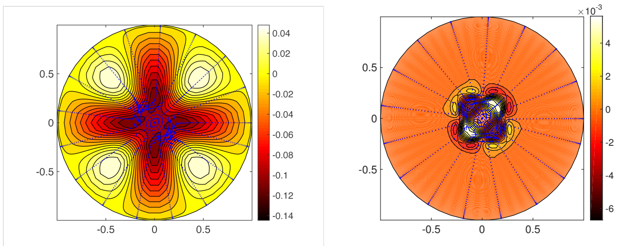

(a) $\mathbf{U}(r,\theta)$ (b) $\mathbf{v}_w(r,\theta,z_0)$

Figure 4: (a)Roll $(U,V,0)$, streak $(0,0,W)$ and (b) (u,v,w) wave profiles at $R = 50000$ for $C2$ at $\alpha = 1.55$. 15 equispaced contour levels are plotted between minimum and maximum (a) $W(r,\theta)$and (b) $w(r,\theta,z_0)$ where min/max taken over (r,θ).

Stability Analysis

Figure 1 shows results of linear stability analysis around the bifurcation points. Note that, even though calculations were carried out upto $R = 50000$, we display solutions upto $R = 14000$ since there is no bifurcation detected beyond $R = 11000$. All solutions, except $C1$, appear through saddle-node bifurcations with 'upper' and 'lower' branches which are observed when an eigenvalue passes through the origin. In all cases we found that there is at least one positive eigenvalues; thus all states are unstable from their onset.

As seen in figure 1, WK, $C2$ solutions are born at about $R = 1658$ and $R = 2300$ respectively. When R increases, lower-branch of WK solution goes through 2 saddle node bifurcations at around $R = 11600$ where it makes an inverse S shape when an unstable real eigenvalue becomes stable, followed by a stability change of a stable eigenvalue. As a side note, this bifurcation is important on its own right because WK solution start exhibiting VWI behaviour with a single dominating axial mode only after this S-shape bifurcations so we could find numerical evidence that supports VWI-theory.

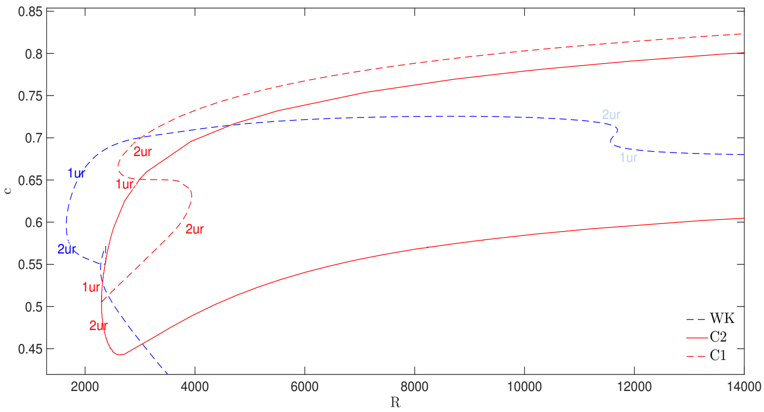

Figure 1: c versus R for WK branch at $\alpha = 1.55$. It should be noted that definition of 'upper' and 'lower' branches are switched as higher wave speed branch has lower energy dissipation. Labels above/below turning points indicate properties of unstable eigenvalues: number of unstable, real-r or complex-c λs.

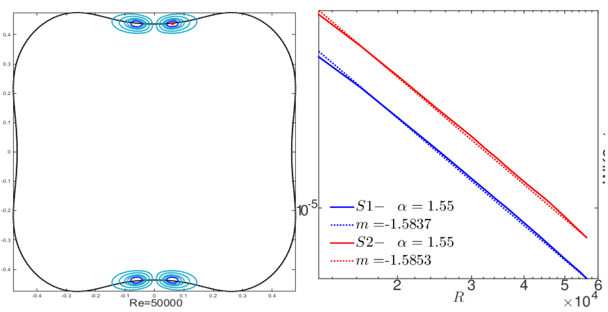

(a) (b)

Figure 5: (a) S_2 contours at $R = 50000$ showing 0.9, 0.8,0.7,0.5 and $0.3\times\ S_{2,m}$. Critical Curve is shown in black, and location of $S_{2,m}$ shown in $*$. (b) Scaling of maximal wave stresses $S_{1,m}$, $S_{2,m}$ with R at $\alpha = 1.55$ for WK.

On the other hand, $C1$ is being created out of $C2$ through another bifurcation which can be seen through linear stability analysis of $C2$ in S-symmetric subspace without imposing additional shift-and-rotate symmetry. As R increases changes in stability of $C1$ is observed as it makes an S shape as seen in figure 1.

Also, we should note that, as you increase R in upper branch some real eigenvalue pairs will join to form a complex pairs, though they are not included here since we only focus on stability around bifurcation points. As a final remark we have recently found new connections on the upper-branch WK solution around $R = 2300$ as seen in figure 1. However, stability calculations are not included here.

Conclusions

In this paper, we report new numerical computations of travelling wave solutions with shift and reflect symmetry through a numerical continuation process. We present some features of these solutions, including scaling of the lower-branch WK with Reynolds number in the range $1.2\times10^4 < R < 5\times10^4$. Quantitative evidence roughly suggests numerically calculated lower-branch WK solution is a finite R realization of VWI states. However, we need larger R calculations in order to achieve scalings that are consistent with asymptotic stress scaling of $R^{-5/3}$ in VWI solutions. It is also worth mentioning that other scalings of WK in the same range give good approximations to expected the R^{-1} scale for rolls, $O(1)$ scale for streaks and a maximal wave amplitude of $O(R^{-5/6})$ of self sustaining process and VWI theory described in [8] & [7].

We also discuss linear stability properties of computes travelling wave solutions near bifurcation points and identify number of unstable directions. We confirmed that these travelling waves have slow and low dimensional unstable manifolds suggesting their relevance to transition in turbulence. It is clear that control of these state are important matters for further research with both theoretical and practical implications.

References

[1] Blackburn, H.M., Hall, P. & Sherwin, S.J., Lower branch equilibria in Couette flow: the emergence of canonical states for arbitrary shear flows. *J. Fluid Mech.*, **726**, 2013, **R2**, 12.

[2] Deguchi, K. & Hall, P., Free-stream coherent structures in parallel boundary-layer flows, *J. Fluid Mech.*, **752**, 2014, 602-625.

[3] Deguchi, K. & Hall, P., Canonical exact coherent structures embedded in high Reynolds number flows, *Phil. Trans. R. Soc*, **A 372**, 2014 , 20130352.

[4] Deguchi, K. & Hall, P., On the instabilities of vortex-wave interaction states, *J. Fluid Mech.*, **is**, 2016.

[5] Faisst, H. & Eckhardt, B. , Traveling waves in pipe flow, *Phys. Rev. Lett.*, **91**, 2003, 224502.

[6] Gibson, J.F., Halcrow, J. & Cvitanovic, P., Equilibrium and travelling-wave solutions of plane Couette flow., *J. Fl. Mech*, **638**,2009, 243-266.

[7] Hall, P. & Sherwin, S.,Streamwise vortices in shear flows: harbingers of transition and the skeleton of coherent structures, *J. Fluid Mech.*, **661**, 2010,178-205

[8] Hall, P. & Smith, F., On strongly nonlinear vortex/wave interactions in boundary layer transition, *J. Fluid Mech.*, **227**, 1991, 641-666.

[9] Hof, B.,van Doorne, C.,Westerweel, J.,Nieuwstadt, F., Faisst, H.,Eckhardt, B.,Wedin, H.,Kerswell, R., & Waleffe, F., Experimental observation of nonlinear traveling waves in the turbulent pipe flow, *Science* **305** (5690), 2004,1594-1598.

[10] Kerswell, R. & Tutty, O., Recurrence of traveling waves in transitional pipe flow, *J. Fluid Mech*, **584**, 2007, 69-102.

[11] Nagata, M., Three dimensional finite-amplitude solutions in plane Coutte flow: bifurcation from infinity, *J. Fluid Mech*, **217**, 1990, 519-527.

[12] Pringle, C.C.T & Kerswell, R.R., Asymmetric, helical and mirror-symmetric travelling waves in pipe flow, *Phys. Rev. Lett.*, **99**, 2007, 074502.

[13] Pringle, C.C.T., Duguet, Y., & Kerswell, R.R., Highly symmetric travelling waves in pipe flow, *Phil. Trans. R. Soc.*, A **367**(1888), 2009, 457-472.

[14] Ozcakir, O. , Tanveer, S. , Hall, P. & Overman E. A. ,Travelling waves in pipe flow, *J. Fluid Mech*, **791**, 2016, 284-328.

[15] Schneider, T. and Eckhardt, B. , Edge States intermediate between laminar and turbulent dynamics in pipe flow, *Phil. Trans. R. Soc.*, A **367**,2009, 577-587.

[16] Viswanath, D.,Recurrent motions within plane Couette turbulence, *J. Fluid Mech*, **580**, 2007, 339-358.

[17] Viswanath, D. & Cvitanovic, P., Stable manifolds and the transition to turbulence in pipe flow., *J. Fluid Mech*, **627**,2009, 215-233.

[18] Waleffe, F., Exact coherent structures in channel flow, *J. Fluid Mech*, **435**, 2001, 93-102.

[19] Waleffe, F., Homotopy of exact coherent structures in plane shear flows, *Phys. Fluids*, **15** (6), 2003,1517-1534.

[20] Wang, J., Gibson, J. & Waleffe, F., Lower branch coherent states in shear flows: transition and control, *Phys. Rev. Lett.*, **98** (20), 2007,204501.

[21] Wedin, H & Kerswell, R., Exact coherent structures in pipe flow: travelling wave solutions, *J. Fluid Mech*, **508**, 2004, 333-371.